Behavioral Modeling of GaN Doherty Power Amplifiers Using Memoryless Polar Domain Functions and Deep Neural Networks

YAHYA KHAWAM, OUALID HAMMI, (Member, IEEE),
LUTFI ALBASHA, (Senior Member, IEEE),
AND HASAN MIR, (Senior Member, IEEE)
Department of Electrical Engineering, College of Engineering, American University of Sharjah, Sharjah, United Arab Emirates

Corresponding author: Lutfi Albasha (lalbasha@aus.edu).

ABSTRACT In this paper, novel Doherty Power Amplifier (DPA) models are presented. The motivation behind the proposed models is to accurately predict static nonlinearities in the compression regions of the carrier and peaking amplifiers. DPAs suffer from a nonlinearity that originates from the carrier amplifier, and a second more pronounced nonlinearity generated at the full compression region following the turn-on of the peaking amplifier. Moreover, these distortions are often observed at different input power levels depending on whether the AM-AM or the AM-PM characteristic is considered. Therefore, the proposed static model is based on independent modeling of the memoryless gain in the polar domain. The static model of the memoryless AM-AM and AM-PM characteristics is augmented with either memory polynomials or deep neural network functions for memory effects modeling. The methodology of building the proposed models and the achieved results are discussed in this paper. The MP based proposed model achieves an NMSE as low as −45.3dB with only 78 model parameters, while the DNN based model achieves an NMSE as low as −46.1dB with only 156 model parameters. However, the DNN based model achieves the best model resilience to changes in the identification data.

INDEX TERMS AM-AM, AM-PM, digital pre-distortion, Doherty power amplifier, linearization, memory effect, polynomial model, deep neural network, bidirectional LSTM, convolutional neural networks.

I. INTRODUCTION

The power amplifier (PA) is a major device included in a transceiver system. Its performance significantly impacts the quality of the transmitted signal and that of the communication link [1]–[4]. Modern PAs are driven by signals having various schemes such as Orthogonal Frequency Division Multiplexing (OFDM). With such advanced schemes, the static and memory effects of the PA should be included in the modeling and linearization processes [5]–[7]. There are many techniques and models developed for linearizing PAs. Each model has a different structure, complexity (number of model parameters) and error performance. Digital Pre-distorters (DPD) and power amplifiers (PA) can be modelled using memory polynomials [5]–[7] as well as neural

networks (NN) [8]–[16]. Real-valued and complex-valued NNs are developed and published in the literature. For example, a real-valued time-delay NN for modeling of 3G base-station PA was developed in [9]. The parameters of the NN were determined by backpropagation method. Different optimization methods can still be used such as particle swarm optimization and genetic algorithm coupled with local minimum search algorithm. The NN model can properly model PA characteristics with satisfactory agreement between simulated and measured data. Also, the dynamic AM-AM and AM-PM can be modelled using the real-valued NN to account for the memory effects. The advantage of using real-valued NNs over complex-valued NNs is that there is no need to use complex-valued backpropagation algorithm to determine the unknown parameters of the model [9]. Other forms of NNs published in the literature include Tapped Advance and Delay Line Neural Net (TADNN) [10]. TADNN models are

The associate editor coordinating the review of this manuscript and approving it for publication was Rocco Giofrè.

based on the feedforward tapped delay line structure. The importance of using the advance taps and the delay taps is to improve the performance of the DPD [10]. It was proven that the TADNN scheme improves PA linearization as compared to conventional delay-tap-only model. A second type of real-valued NN is the Two Layer Artificial Neural Network (2LANN) [11]. This model was developed for pico-cell PAs which output about 2 watts or less. The motivation behind this NN is to realize a model which can be efficiently implemented in a real-time application with hardware considerations. The 2LANN model provides acceptable performance with significant reduction in computational resources. A different approach for using NN in PA modelling is described in [12]. It is a real-valued autoregressive with exogenous input NN which can model a PA with memory effects. Complex-valued NN are also developed in the literature. A complex-valued two hidden layers NN (2HLANN) was published in [13]. Furthermore, a recurrent neural network termed the instant gated recurrent neural network (IGRNN) was developed in [14]. Bidirectional long-short-term memory networks (BiLSTM) have been introduced in the literature [15]. This architecture outperforms many current deep learning techniques for DPD and PA modeling especially when the PA exhibits strong memory effects. Furthermore, convolutional neural networks (ConvNet) have been also shown in the literature to be effective for modeling PA behavior [16]. The ConvNet model was found to reduce model complexity by more than 50% as compared to other deep learning techniques [16].

Other types of DPD and PA models are based on the memory polynomial models (MP). Unlike NN models, MPs are a subset of the Volterra series commonly used to lower the complexity of the models [17]–[23]. Also, memory polynomials have been used as part of multi-box structures to achieve high accuracy with lower model complexity than the standalone memory polynomial model [24], [25].

In this paper, new behavioral models dedicated for high efficiency Doherty power amplifiers (DPAs) are introduced. This is of prime importance since many of power amplification systems deployed in base stations are based on the DPA architecture. In fact, power efficiency of wireless communication systems is an essential part in the green communication systems. However, achieving high DPA efficiency introduces strong nonlinear effects due to the efficiency-linearity dilemma in PAs. Since linearity is a must for avoiding adjacent channels interferences, efficient amplification along with excellent linearization technique must be implemented. Many models in the literature deal with the PA modelling problem as a unified black-box model. Meaning, equations are used to determine the behavior of the PA along with its memory effects based on the measured input and output data. Those models range from different forms of complex-valued polynomial models to real-valued neural network-based models. The issue is that different PAs have different levels of memory effects. As such, when running an optimization algorithm, large number of fitting

parameters can contribute to memory effects even though a PA's memory effect might be mild. In contrast, a large number of parameters related to memory effects would contribute to static characteristics of the PA. Optimization algorithms like genetic algorithm and particle swarm can only guarantee convergence to global minimum error without understanding the physical relevance of the parameters being optimized. Therefore, a certain number of parameters will exist in the model that does not affect the overall performance of the PA model while unnecessarily increasing the model complexity. The principal contributions of this paper are as follows:

1) Develop low complexity and high performance models for the memoryless AM-AM and AM-PM characteristics of GaN based DPA.
2) Integrate the static AM-AM and AM-PM models with memory effects functions to further enhance the modeled characteristics of the DPA. Two methods are proposed for integrating the static models along with the memory effects. The first method uses memory polynomials, and the second employs a deep neural network (DNN).
3) The proposed DPA models are more resilient, in the sense that their accuracies remain superior to the state of the art models following variations in the validation waveform.
4) When MP is used to model the memory effects of the device under test (DUT), the proposed model achieves more than 8dB enhancement in the normalized mean squared error (NMSE) at similar complexity when compared to state of the art MP models.
5) The use of DNN to model the dynamic distortions allows the proposed model to outperform standard NN models by approximately 3dB in the NMSE while having 85% to 90% less complexity.

The paper is organized as follows: first the proposed DPA models will be discussed. Then, the proposed modeling process is described and the obtained results are reported and discussed.

II. PROPOSED MODELING OF DPA

The nonlinearity at the compression point of the PA must be compensated for a device operating at reasonably high efficiency. A second nonlinearity exists in DPA that further worsen the linearity performance. Typically, a DPA is designed using Class AB and Class C amplifiers serving as the carrier and the peaking amplifiers, respectively. At relatively low input power, the Class AB amplifier becomes the dominant operator in the DPA. When input power reaches the compression point of the Class AB amplifier, Class C starts contributing to the output power of the DPA using load modulation. The second nonlinearity exists when both the class AB and class C PAs contribute to the output power.

The power characteristic of a DPA can be divided into several regions: first is Class AB linear region followed by Class
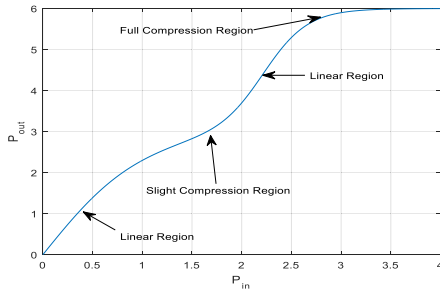
FIGURE 1. Example of DPA power characteristic illustrating two typical transitions. The first transition is due to the compression of the carrier amplifier around the turn-on point of the peaking amplifier, the second is due to the compression of the Doherty PA operating at full power capabilities.

AB compression region. Then, Class C turn-on region, and finally Class C compression occurs. This nonlinear behavior is depicted in Figure 1. Therefore, a model should predict Class C turn-on effect to comprehensively predict the behavior of the DPA.

A. STATIC DISTORTIONS MODELING

The static distortions sub-model is designed to have the ability to model the specific nonlinearity profile of DPA which commonly includes two inflection points as depicted in Figure 1. Furthermore, the proposed static model predicts the complex-valued gain behavior of the DPA by decoupling the AM-AM and AM-PM distortions. Equations (1) to (5) show the mathematical model for the complex-valued static gain, G_{PA}, and the predicted signal, x_{out_SD}, at the output of the static distortions model.

$$\left| G_{PA,n} \right| = a_1 - a_2 e^{-\left(\frac{|x_n| - a_3}{a_4} \right)^2} - \frac{a_5}{1 + e^{-a_6(|x_n| - a_7)}} \quad (1)$$

$$\angle G_{PA,n} = -b_4 + b_5 e^{b_6 f_n} + b_7 e^{b_8 |x_n| - b_9} \quad (2)$$

$$f_n = b_1 |x_n| - 0.5 \left[b_1 |x_n| + \sqrt{(b_1 |x_n| - b_2)^2 + b_3} \right. $$
$$\left. - \sqrt{b_2 + b_3} \right] \quad (3)$$

$$G_{PA,n} = \left| G_{PA,n} \right| \angle G_{PA,n} \quad (4)$$

$$x_{out\_SD,n} = \left(\left| G_{PA,n} \right| \angle G_{PA,n} \right) \cdot x_n \quad (5)$$

a_1 through a_7, and b_1 through b_9 are real-valued fitting parameters, and x_n is the complex-valued input sample at time instant n. One of the advantages of using the proposed model is that the number of parameters used in modeling the static characteristics of the DUT is always constant (16 parameters) regardless of the DPA used. This is true as long as the DPA exhibits the nonlinearity profile shown in Figure 1 which is standard for all high-efficiency DPA designs.

A careful examination of the AM-AM and AM-PM characteristics of Gallium Nitride (GaN) based Doherty power amplifiers brings to light a key observation: the inflection points of the AM-AM and AM-PM characteristics do not occur at the same input power levels. This behavioural misalignment in the distortions profiles of the AM-AM and

AM-PM characteristics of GaN Doherty power amplifiers is not specific to the considered DUT but can be observed in several designs reported in the literature [25]–[28]. Therefore, it is anticipated that modelling the static AM-AM and AM-PM characteristics separately will enable a better independent control on the distortions profile and consequently lead to enhanced performance. In the proposed model, the independent modelling of the AM-AM and AM-PM characteristics is implemented using real-numbers based fitting parameters to model each specific characteristic of the DPA without affecting the other one. For example, fitting parameters in the proposed AM-AM model in Equation (1) do not affect AM-PM conversion characteristic. Also, fitting parameters in the proposed AM-PM conversion in Equations (2) and (3) do not affect the AM-AM characteristic of the DPA. Meaning, each characteristic can be separately modeled.

B. STATIC DISTORTIONS/MEMORY POLYNOMIALS MODEL

The proposed static distortions model is not suitable on its own, since modern PAs unavoidably exhibit memory effects. Hence, residual nonlinearities are expected between the measured output signal and the estimated signal at the output of the static distortion function. This residual memory effects signal is given by:

$$x_{out\_ME,n} = x_{out\_meas,n} - x_{out\_SD,n} \quad (6)$$

where $x_{out\_meas,n}$ is the measured output sample of the device under test.

In order to augment the proposed static model, a first configuration is proposed by combining the static distortions sub-model with a memory polynomials sub-model in order to accurately mimic the behavior of the Doherty amplifier. This augmented model is referred to as the SMP model (Static and Memory Polynomial model) since the static model output obtained from (5) is coupled with the memory polynomial output which augments the static model by including the memory effect as illustrated in Figure 2. The overall output of the SMP model is given by:

$$x_{out\_SMP,n} = x_{out\_SD,n} + x_{out\_MP,n} \quad (7)$$

The output samples $x_{out\_MP,n}$ of the memory polynomial is calculated using:

$$x_{out\_MP,n} = \sum_{k=k_{min}}^{M_{MP}} \sum_{j=1}^{N_{MP}} h_{jk} x_{n-k} |x_{n-k}|^{j-1} \quad (8)$$

h_{jk} are the complex-valued model parameters of the MP sub-model. The complexity of the memory effects is controlled by the dimensions (nonlinearity order N_{MP} and memory depth M_{MP}) chosen in Equation (8). It is important to note here that the MP function used in this model does not include the static term (hence $k_{min} = 1$). This is to avoid redundancy since the static behavior is already modeled by the proposed static AM-AM and AM-PM functions.
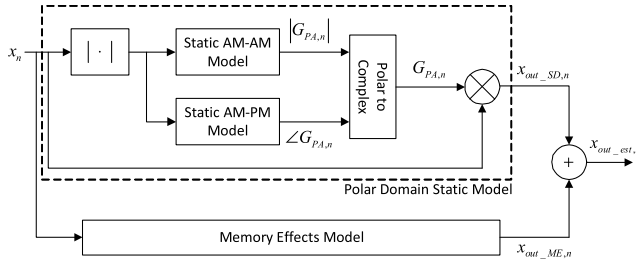
FIGURE 2. Block diagram of the proposed model for GaN DPA. Polar domain static model output is combined with the memory effects model output to estimate the DUT's output signal. Memory effects model can be a memory polynomial or a deep neural network.
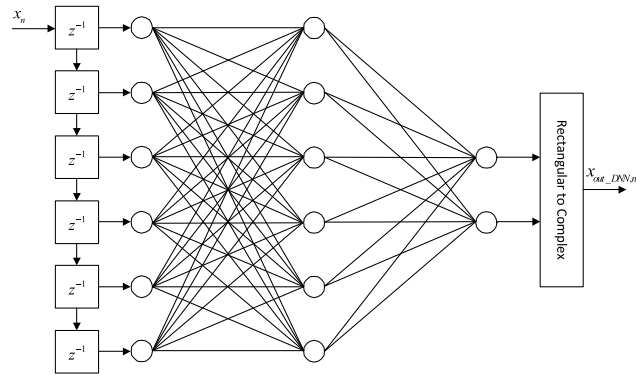

FIGURE 3. Deep neural network model used to model the DUT's memory effects in the SDNN model.

C. STATIC DISTORTIONS/DEEP NEURAL NETWORK MODEL

The second model proposed in this work shares similarity with the first model in the sense that the same static distortions sub-model is used for the accurate modeling of the DPA memoryless nonlinearity profile, however, a different sub-model is introduced for the modeling of the memory effects of the device under test. In this SDNN model (Static and Deep Neural Network model), the static distortions modeling is performed in the same way as the SMP model reported in the previous sub-section. However, a deep neural network (DNN) is used to model the memory effects instead of the memory polynomials used in the SMP model. The block diagram describing the DNN sub-model is shown in Figure 3. In this work, the DNN used has four layers: an input layer, two hidden layers and one output layer. The activation function used is a tanh function. Multiple activation functions other than tanh functions were tested, but they did not provide a usable model convergence. The input consists of 6 delays of the input x_n, 6 neurons per hidden layer and two outputs for in-phase and quadrature components. The output of the static model $(x_{out\_SD,n})$ and the output of the neural network $(x_{out\_DNN,n})$ are added together to yield the predicted output sample of the DPA. This model was optimized using the Keras API of TensorFlow platform for machine learning. The advantage for using a neural network rather than memory polynomial functions for modeling the memory effects will be discussed in the next section while assessing the relative performances of the two proposed models.

III. DISCUSSION AND RESULTS

In order to develop the proposed models, the static model should be separately identified, then the memory effects model will be derived. The identification process of the entire model is as follows:

1) Extract the memoryless AM-AM and AM-PM characteristics of the device under test by processing the raw measured data. This includes the steps commonly used in the identification of two-box models such as the augmented-Wiener, the Augmented-Hammerstein, and twin-nonlinear two-box models. These intermediate steps are namely time-delay alignment between the input and output waveform, data averaging to eliminate memory effects, and finally calculation of the memoryless gain magnitude and phase by using the averaged time-aligned versions of the measured input and output baseband complex waveforms.
2) Apply fitting algorithm to calculate the parameters of the static AM-AM model (a_1 through a_7) from equation (1),
3) Apply fitting algorithm to calculate the parameters of the static AM-PM model (b_1 through b_9) from equations (2) and (3).
4) Use Equations (5) and (6) to de-embed the measurement data and obtain the desired complex output signal of the memory effects modelling function x_{out_ME}.
5) Identify the parameters of the second sub-model using the input signal and the desired sub-model output signal (x_{out_ME}). This step differs whether the model being identified is the SMP or the SDNN.

The flowchart in Figure 4 summarizes the parameters identification process described above. As it is the case for any behavioral model, the derived coefficients and the model accuracy is only valid for the observed behavior. Variations in the test signal or operating conditions which will emulate a different behavior would require a new identification of the model coefficients as per the steps described above. This is common to any behavioral model and does not affect the generality of the proposed model.

For the experimental validation of the proposed model, a Doherty PA (DPA) employing a 10W GaN transistor is used as the device under test. In this DUT, the carrier amplifier was optimized for efficiency using harmonic tuning. The PA operates in the 2425MHz frequency range. The DUT was driven by a 20MHz long term evolution (LTE) test signal having a peak to average power ration (PAPR) of 9.7dB. The instantaneous input and output baseband complex waveforms were acquired using the standard setup for power amplifiers characterization using modulated test signals [5] in which an arbitrary waveform generator was used to generate the RF test signal applied at the input of the DUT. The output signal was attenuated and then digitized using a commercial vector signal analyzer.

The measured AM-AM and AM-PM characteristics of the DUT as well as their estimated static versions are reported
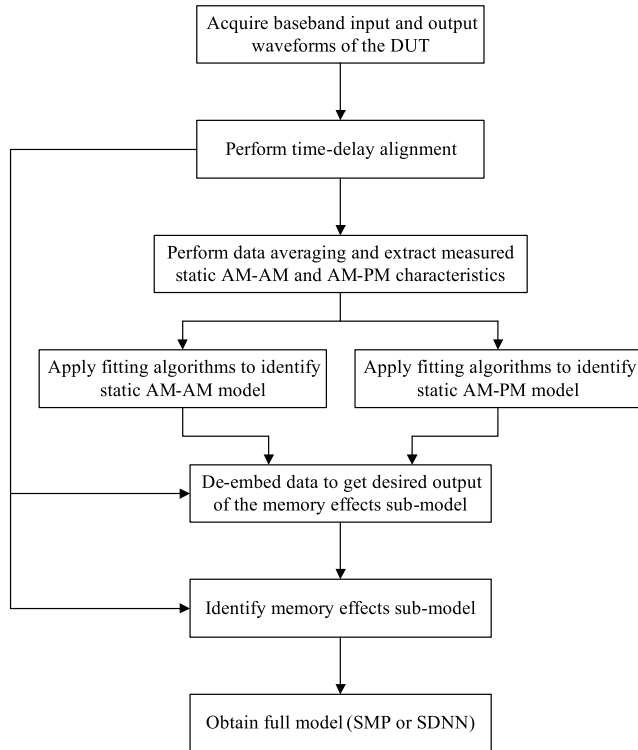
FIGURE 4. Flow chart of the static model identification and the SMP and SDNN models identifications.

in Figure 5. This figure demonstrated the ability of the static model to mimic the nonlinear behavior of the AM-AM and AM-PM characteristics. Furthermore, it appears that, for the considered device under test, a first inflection point in the AM-AM characteristic occurs at an input power around −26dBm. However, the first inflection point in the AM-PM characteristic is observed when the input power level is around −23dBm. Similarly, the second inflection point of the AM-AM characteristic corresponds to an input power level of approximately −20dBm, while that of the AM-PM appears at around −16dBm. This confirms the suitability of an independent modelling of the AM-AM and AM-PM characteristics at origin of the proposed static distortions model.

The formulation of the static functions proposed to model the AM-AM and the AM-PM characteristics emanated from the following observations. For the AM-AM model:

- Fitting parameter a_1 represents the constant gain of the DPA at very low input power (−50 to −45dBm region for this DUT). This typically corresponds to the small signal gain of the carrier amplifier.
- In the very high input power region where both amplifiers are on and the second compression starts (−20 to −15dBm for the DUT), the gain exponentially decreases due to saturation of the DPA. Therefore, a sigmoid function is used to model the saturation of the DPA. Fitting parameters a_5 and a_6 represent the level and the rate of the gain decay, respectively. Fitting parameter a_7 represents the input power at which the gain starts to exponentially decrease.
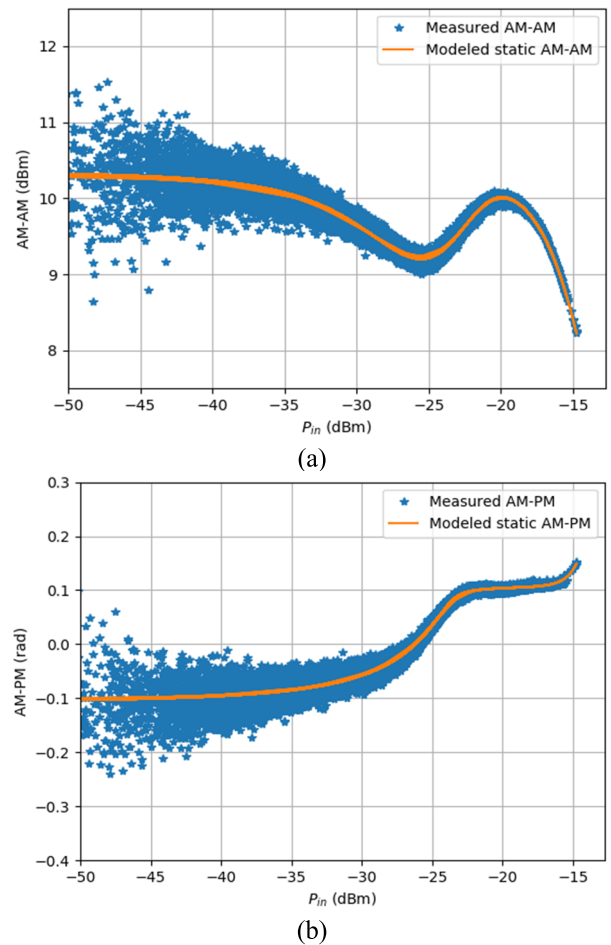

(a)

(b)

FIGURE 5. Measured AM-AM and AM-PM characteristics and their estimated static versions. (a) AM-AM characteristic, (b) AM-PM characteristic.

- In the middle input power region (−45 to −20dBm for the DUT), the gain decreases (from −45 to −25dBm for the DUT) and then increases again (from −25 to −20dBm for the DUT) due to the compression of the main amplifier followed by the turn-on of the peaking amplifier. This is modelled using a bell-shaped function to mimic the decrease and increase of the gain at this region. Fitting parameter a_2 represents the amount of gain decrease in this transition region while fitting parameter a_3 represents the input power at which the peaking amplifier starts contributing to the DPA output power.

The reasons behind the proposed formulation of the static AM-PM model are as follows:

- Fitting parameter $−b_4$ represents the constant phase distortion of the carrier amplifier of the DPA at low input power (−50 to −40dBm for the DUT).
- Then phase distortion starts to increase due to gain compression of the carrier amplifier (−40 to −23dBm for the DUT). This modelled using an exponential function. Fitting parameter b_5 represents the level of the increase of the phase distortion in the carrier amplifier in this
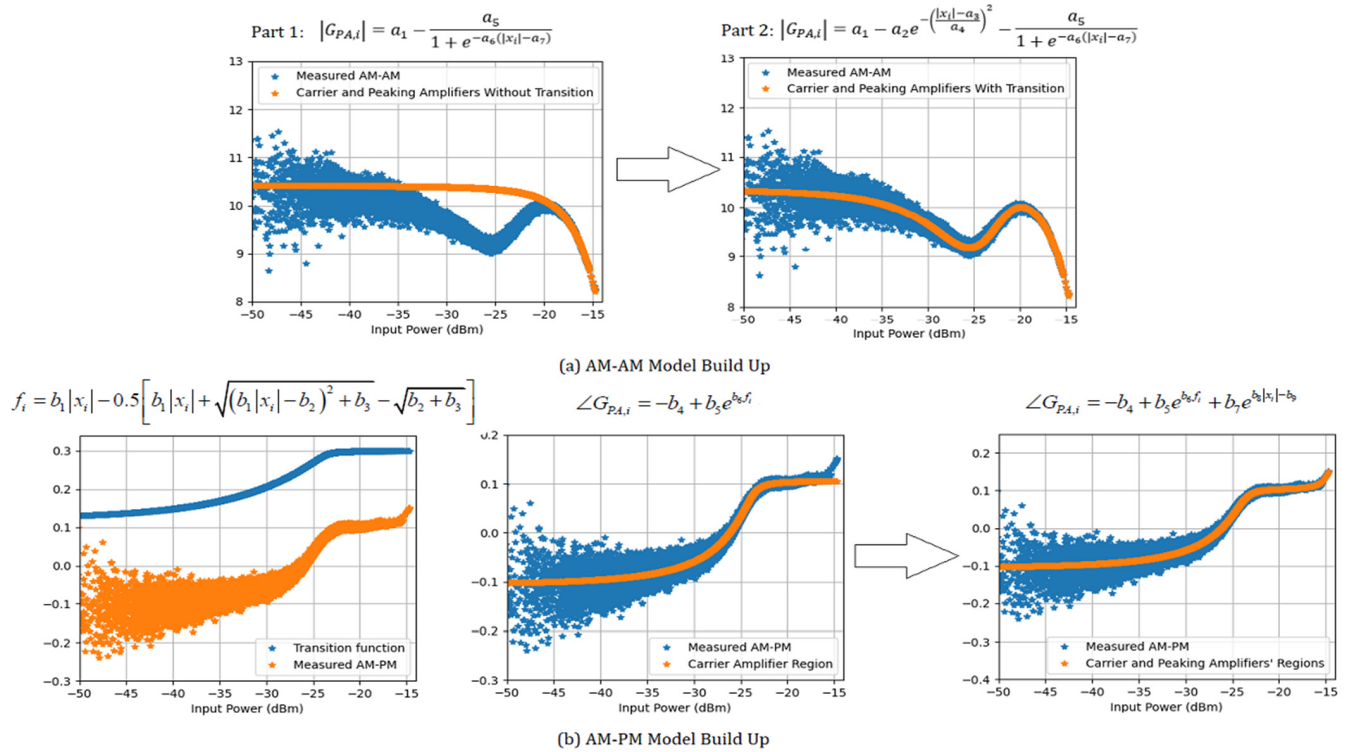
Part 1: $|G_{PA,i}| = a_1 - \dfrac{a_5}{1+e^{-a_6(|x_i|-a_7)}}$

Part 2: $|G_{PA,i}| = a_1 - a_2 e^{-\left(\frac{|x_i|-a_3}{a_4}\right)^2} - \dfrac{a_5}{1+e^{-a_6(|x_i|-a_7)}}$

(a) AM-AM Model Build Up

$f_i = b_1|x_i| - 0.5\left[b_1|x_i| + \sqrt{(b_1|x_i|-b_2)^2 + b_3} - \sqrt{b_2+b_3}\right]$

$\angle G_{PA,i} = -b_4 + b_5 e^{b_6 f_i}$

$\angle G_{PA,i} = -b_4 + b_5 e^{b_6 f_i} + b_7 e^{b_8|x_i|-b_9}$

(b) AM-PM Model Build Up

FIGURE 6. Breakdown of the static AM-AM and AM-PM models (a) AM-AM and (b) AM-PM.

power region. Fitting parameter b_6 represent the rate of rise of phase distortion.

- At higher input power (more than -25dBm for the DUT), the peaking amplifier kicks in, and the effect of the carrier amplifier starts to diminish. Therefore, a function is needed to start suppressing the phase distortion of the carrier amplifier. In this work, transition function as formulated in Equation (3) is used to do so. This function, f_i, has three fitting parameters: b_1 which represents how fast this transition functions saturates, b_2 represents the level of saturation, and b_3 is the knee point for the transition function.
- To model the effect of the peaking amplifier compression (from -23 to -15dBm for the DUT), a second exponential function is used to model the phase distortion. This part has three fitting parameters: b_7 represents the level of the increase of the phase distortion in this power region, b_8 represent the rate of rise of the phase distortion, and b_9 represents the input power at which the peaking amplifier kicks in.

The AM-AM and AM-PM models' build-up is depicted in Figure 6. This figure clearly illustrates the effect of each term in Equations (1) and (2) and their respective contributions to recreating the AM-AM and AM-PM distortions behavior. Once the static distortions model is built, the input and output signals of the dynamic distortions functions are de-embedded.

First, the performance of the proposed SMP model was assessed. In this case, the nonlinearity order and memory

depth of the polynomial function were set to $N_{MP} = 6$ and $M_{MP} = 6$, respectively. The modeled AM-AM and AM-PM characteristics are reported in Figure 7 and 8, respectively. These figures show the ability of the proposed model in mimicking the actual behavior of the DUT.

In order to benchmark the performance of the proposed model against previously reported state of the art model, the NMSE was used. The NMSE is commonly used to benchmark the performance of behavioral models, and as is defined as:

$$NMSE_{dB} = 10\log_{10}\frac{\sum_{i=1}^{L}\left|x_{out\_meas,i} - x_{out\_est,i}\right|^2}{\sum_{i=1}^{L}\left|x_{out\_meas,i}\right|^2} \quad (9)$$

where L refers to the number of samples used for calculating the NMSE. $x_{out\_meas,i}$ and $x_{out\_est,i}$ are the ith measured and estimated output samples of the validation waveforms, respectively.

The NMSE was calculated using 40,000 samples. The training NMSE refers to the NMSE obtained when the validation waveform is the same as the waveform used to train the model.

The SMP model was benchmarked against several comparable models including the standalone MP model, the EMP model [21], and a hybrid model made of the combination of the MP and EMP models [29]. The training NMSE results reported in Table 1 clearly demonstrate the effectiveness and superiority of the proposed model as it achieves significantly
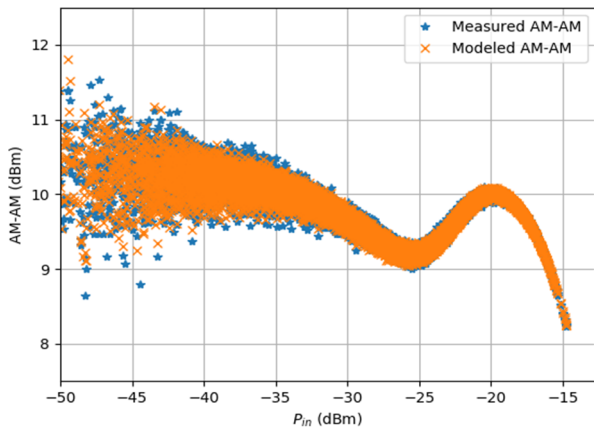
FIGURE 7. Measured and modeled AM-AM characteristic of the DUT. The modeled characteristic is the one obtained using the SMP model.
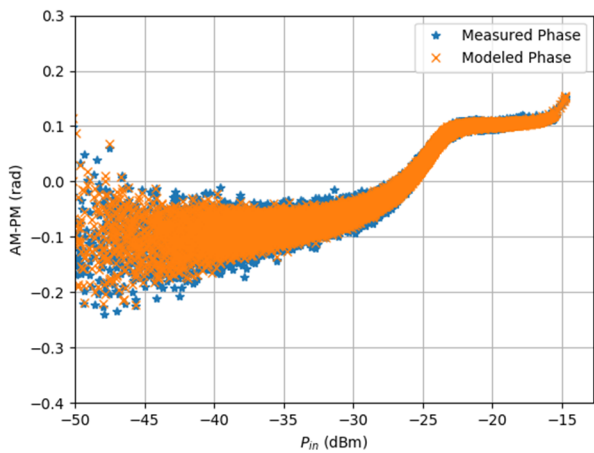

FIGURE 8. Measured and modeled AM-PM characteristic of the DUT. The modeled characteristic is the one obtained using the SMP model.

TABLE 1. Benchmarking of SMP Model against State of Art MP-Based Models.

Model	Model Complexity	NMSE (dB)
MP $\left(M_{MP} = N_{MP} = 6\right)$	84	-37.5
EMP $\left(M_{EMP} = N_{EMP} = 6\right)$	84	-33.6
EMP+MP$\big|_{k \neq 0}$ $\left(M_{MP} = M_{MP} = 4\right)$ $\left(N_{MP} = N_{MP} = 6\right)$	108	-32.9
SMP $M_{MP} = N_{MP} = 6$	**76**	**-45.3**

lower NMSE than the benchmark models while using comparable number of parameters. Indeed, the proposed SMP model reduces the NMSE by approximately 8 to 12dB as reported in Table 1.

The SDNN model was also compared to other state of the art neural network based models. The parameters of the

TABLE 2. Benchmarking of SDNN Model against State of Art NN-Based Models.

Model	Model Complexity	NMSE (dB)
BiLSTM [24] (7 taps input layer, 2 BiLSTM layers + 2 Dense layers + 1 output layer)	2134	-42.1
ConvNet [25] (7 taps input layer, 1 Conv layer + 1 flatten layer + 2 dense layers + 1 output layer)	992	-42.3
DNN [9] (14 taps input layer, 3 dense layers, 1 output layer)	1182	-37.1
SDNN	**156**	**-46.1**

TABLE 3. Benchmarking of SDNN Model against State of Art NN-Based Models.

	Offset frequency	Measured at the DUT output	Estimated using SDNN model
ACLR 1	−20MHz	−30.7dBC	−30.6dBC
	+20MHz	−30.7dBC	−30.6dBC
ACLR 2	−40MHz	−44.0dBC	−43.9dBC
	+40MHz	−43.3dBC	−43.6dBC

DNN used in the SDNN are the same as those described in section II. In table 2, the training NMSE of the proposed SDNN model is compared to that of the NN based models reported in [9], [24] and [25]. The results reported in this Table reveal the ability of the proposed SDNN model in achieving lower NMSE while requiring significantly less parameters resulting in between 85% and 90% less complexity without compromising the model accuracy. To further assess the accuracy of the SDNN model and its ability to accurately predicted the amplifier's output signal, the measured spectrum at the output of the DUT as well as the estimated spectrum at the output of the SDNN model are reported in Figure 9. These plots corroborate the accuracy of the SDNN model as expected by its NMSE performance. Moreover, the adjacent channel leakage ratio (ACLR) was calculated at the output of the DUT and its SDNN model. These results reported in Table 3 confirm the accuracy of the model and its ability to precisely predict the behavior of the DUT in time domain (as confirmed by the NMSE results) and frequency domain (as illustrated by spectra and ACLR data).

Furthermore, to evaluate the robustness of the considered models, 10 other waveforms (different from the training waveform) were used to validate the models. The original test signal contained 200,000 samples, 40,000 of which were used to train the models. The 10 validation waveforms were selected as part of the remaining 160,000 samples of the test waveforms that were not used to train the model. Hence, a total of 11 NMSE values (1 training NMSE and 10 validation NMSE) were calculated for each model. The results of this robustness assessment are summarized in Figure 10. This figure reports the training NMSE for each model, as well as
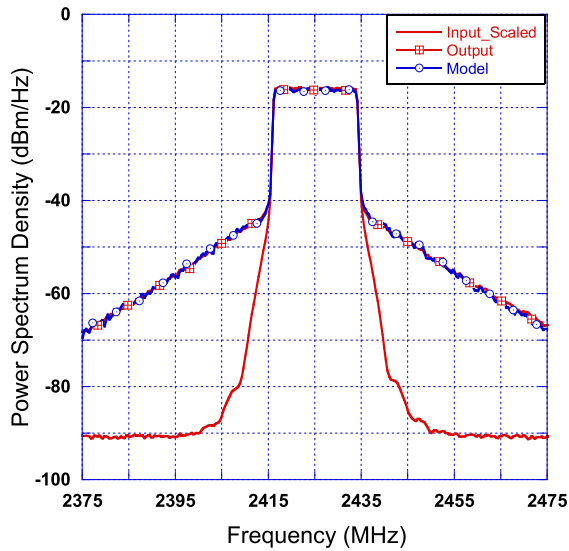
FIGURE 9. Measured spectrum at the output of the DUT and estimated spectrum using the SDNN model.
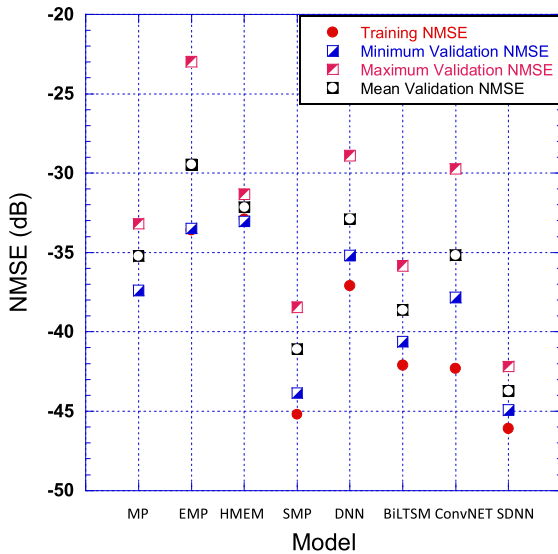

FIGURE 10. Performance benchmarking of the proposed SMP and SDNN models. The training NMSE, and minimum, maximum and mean validation NMSE for 10 validation datasets are reported. Proposed models consistently outperforming state of the art models.

the maximum, minimum and mean validation NMSE of each model based on the results of the 10 validation waveform. For consistency of the results, the same 10 validation waveforms were applied to all models. Based on this data, it appears that the proposed SMP and SDNN models outperform all other models. Moreover, the SDNN models has a better robustness than the SMP model as it can be observed by the reduced NMSE variation following changes in the validation signals. However, this is achieved at the expense of a higher model complexity.

IV. CONCLUSION

In this paper, novel behavioral models dedicated for GaN based Doherty power amplifiers were proposed. The novelty resides in the use of novel polar domain independent

modeling of the static distortions of the DUT. For this purpose, independent functions were used to model the memoryless AM-AM and AM-PM characteristics of the device under test. This enabled a more accurate modeling of the two distortions profiles which showed inflection points occurring at different input power levels. The proposed static distortions model was then augmented with a memory polynomials, and later by a DNN function. Experimental validation demonstrated that the proposed models achieved better NMSE than comparable state of the art models. The proposed SMP model achieved between 8 and 10dBs better NMSE than its previously reported counterparts. Furthermore, the SDNN model led to slight NMSE enhancement compared to other NN based models but up to 90% reduction in the model complexity. Finally, a study of the robustness of the proposed models was carried out and showed that the performance of the SDNN model is less sensitive to variations in the validation signal than that of the SMP model.

REFERENCES

[1] T. Qi and S. He, "Power up potential power amplifier technologies for 5G applications," *IEEE Microw. Mag.*, vol. 20, no. 6, pp. 89–101, Jun. 2019.

[2] L. Albasha, C. Clifton, Y. Jingu, A. Lawrenson, H. Motoyama, S. Bensmida, K. A. Morris, and K. Kohama, "An ultra-wideband digitally programmable power amplifier with efficiency enhancement for cellular and emerging wireless communication standards," *IEEE Trans. Circuits Syst. I, Reg. Papers*, vol. 63, no. 10, pp. 1579–1591, Oct. 2016.

[3] F. M. Ghannouchi, "Power amplifier and transmitter architectures for software defined radio systems," *IEEE Circuits Syst. Mag.*, vol. 10, no. 4, pp. 56–63, Nov. 2010.

[4] R. Ma, K. H. Teo, S. Shinjo, K. Yamanaka, and P. M. Asbeck, "A GaN PA for 4G LTE-advanced and 5G: Meeting the telecommunication needs of various vertical sectors including automobiles, robotics, health care, factory automation, agriculture, education, and more," *IEEE Microw. Mag.*, vol. 18, no. 7, pp. 77–85, Nov. 2017.

[5] F. M. Ghannouchi, O. Hammi, and M. Helaoui, *Behavioral Modeling and Predistortion of Wideband Wireless Transmitters*. Chichester, U.K.: Wiley, 2015.

[6] A. Katz, J. Wood, and D. Chokola, "The evolution of PA linearization: From classic feedforward and feedback through analog and digital predistortion," *IEEE Microw. Mag.*, vol. 17, no. 2, pp. 32–40, Feb. 2016.

[7] F. M. Ghannouchi and O. Hammi, "Behavioral modeling and predistortion," *IEEE Microw. Mag.*, vol. 10, no. 7, pp. 52–64, Dec. 2009.

[8] Y. Khawam, L. Albasha, and H. Mir, "Accurate and low complexity polynomial and neural network models for PA digital pre-distortion," in *Proc. 16th Medit. Microw. Symp. (MMS)*, Abu Dhabi, United Arab Emirates, Nov. 2016, pp. 1–4.

[9] T. Liu, S. Boumaiza, and F. M. Ghannouchi, "Dynamic behavioral modeling of 3G power amplifiers using real-valued time-delay neural networks," *IEEE Trans. Microw. Theory Techn.*, vol. 52, no. 3, pp. 1025–1033, Mar. 2004.

[10] T. Gotthans, G. Baudoin, and A. Mbaye, "Digital predistortion with advance/delay neural network and comparison with Volterra derived models," in *Proc. IEEE 25th Annu. Int. Symp. Pers., Indoor, Mobile Radio Commun. (PIMRC)*, Washington, DC, USA, Sep. 2014, pp. 811–815.

[11] M. K. Ngwar and J. S. Wight, "An artificial neural network for wideband pre-distortion of efficient pico-cell power amplifiers," in *Proc. 6th Int. Symp. Commun., Control Signal Process. (ISCCSP)*, Athens, Greece, May 2014, pp. 562–565.

[12] L. M. Aguilar-Lobo, J. R. Loo-Yau, S. Ortega-Cisneros, P. Moreno, and J. A. Reynoso-Hernandez, "Experimental study of the capabilities of the real-valued NARX neural network for behavioral modeling of multistandard RF power amplifier," in *IEEE MTT-S Int. Microw. Symp. Dig.*, Phoenix, AZ, USA, May 2015, pp. 1–4.

[13] F. Mkadem and S. Boumaiza, "Physically inspired neural network model for RF power amplifier behavioral modeling and digital predistortion," *IEEE Trans. Microw. Theory Techn.*, vol. 59, no. 4, pp. 913–923, Apr. 2011.

[14] G. Li, Y. Zhang, H. Li, W. Qiao, and F. Liu, "Instant gated recurrent neural network behavioral model for digital predistortion of RF power amplifiers," *IEEE Access*, vol. 8, pp. 67474–67483, 2020.

[15] J. Sun, W. Shi, Z. Yang, J. Yang, and G. Gui, "Behavioral modeling and linearization of wideband RF power amplifiers using BiLSTM networks for 5G wireless systems," *IEEE Trans. Veh. Technol.*, vol. 68, no. 11, pp. 10348–10356, Nov. 2019.

[16] X. Hu, Z. Liu, X. Yu, Y. Zhao, W. Chen, B. Hu, X. Du, X. Li, M. Helaoui, W. Wang, and F. M. Ghannouchi, "Convolutional neural network for behavioral modeling and predistortion of wideband power amplifiers," 2020, *arXiv:2005.09848*. [Online]. Available: http://arxiv.org/abs/2005.09848

[17] J. Kim and K. Konstantinou, "Digital predistortion of wideband signals based on power amplifier model with memory," *Electron. Lett.*, vol. 37, no. 23, pp. 1417–1418, Nov. 2001.

[18] D. R. Morgan, Z. Ma, J. Kim, M. G. Zierdt, and J. Pastalan, "A generalized memory polynomial model for digital predistortion of RF power amplifiers," *IEEE Trans. Signal Process.*, vol. 54, no. 10, pp. 3852–3860, Oct. 2006.

[19] V. N. Manyam, D. G. Pham, C. Jabbour, and P. Desgreys, "An FIR memory polynomial predistorter for wideband RF power amplifiers," in *Proc. IEEE Int. New Circuits Syst. Conf.*, Strasbourg, France, Jun. 2017, pp. 249–252.

[20] S. Lajnef, N. Boulejfen, A. Abdelhafiz, and F. M. Ghannouchi, "Two-dimensional Cartesian memory polynomial model for nonlinearity and I/Q imperfection compensation in concurrent dual-band transmitters," *IEEE Trans. Circuits Syst. II, Exp. Briefs*, vol. 63, no. 1, pp. 14–18, Jan. 2016.

[21] O. Hammi, F. M. Ghannouchi, and B. Vassilakis, "A compact envelope-memory polynomial for RF transmitters modeling with application to baseband and RF-digital predistortion," *IEEE Microw. Wireless Compon. Lett.*, vol. 18, no. 5, pp. 359–361, May 2008.

[22] H. Li, Y. Zhang, G. Li, and F. Liu, "Vector decomposed long short-term memory model for behavioral modeling and digital predistortion for wideband RF power amplifiers," *IEEE Access*, vol. 8, pp. 63780–63789, 2020.

[23] J. Ren, "A new digital predistortion algorithms scheme of feedback FIR cross-term memory polynomial model for short-wave power amplifier," *IEEE Access*, vol. 8, pp. 38327–38332, 2020.

[24] O. Hammi and F. M. Ghannouchi, "Twin nonlinear two-box models for power amplifiers and transmitters exhibiting memory effects with application to digital predistortion," *IEEE Microw. Wireless Compon. Lett.*, vol. 19, no. 8, pp. 530–532, Aug. 2009.

[25] M. Younes, O. Hammi, A. Kwan, and F. M. Ghannouchi, "An accurate complexity-reduced 'PLUME' model for behavioral modeling and digital predistortion of RF power amplifiers," *IEEE Trans. Ind. Electron.*, vol. 58, no. 4, pp. 1397–1405, Apr. 2011.

[26] W. Hallberg, M. Ozen, D. Gustafsson, K. Buisman, and C. Fager, "A Doherty power amplifier design method for improved efficiency and linearity," *IEEE Trans. Microw. Theory Techn.*, vol. 64, no. 12, pp. 4491–4504, Dec. 2016.

[27] H. Huang, J. Xia, A. Islam, E. Ng, P. M. Levine, and S. Boumaiza, "Digitally assisted analog/RF predistorter with a small-signal-assisted parameter identification algorithm," *IEEE Trans. Microw. Theory Techn.*, vol. 63, no. 12, pp. 4297–4305, Dec. 2015.

[28] I. Kim, J. Moon, S. Jee, and B. Kim, "Optimized design of a highly efficient three-stage Doherty PA using gate adaptation," *IEEE Trans. Microw. Theory Techn.*, vol. 58, no. 10, pp. 2562–2574, Oct. 2010.

[29] O. Hammi, M. Younes, and F. M. Ghannouchi, "Metrics and methods for benchmarking of RF transmitter behavioral models with application to the development of a hybrid memory polynomial model," *IEEE Trans. Broadcast.*, vol. 56, no. 3, pp. 350–357, Sep. 2010.

YAHYA KHAWAM received the bachelor's and master's degrees from the American University of Sharjah, in 2012 and 2016, respectively. While studying for his bachelor's degree, he published two articles regarding the Lithium-ion battery charger circuit and blood glucose measurements using transmission spectroscopy. In 2013, he was awarded graduate teaching assistance (GTA) from the Master of Science in Electrical Engineering (MSEE) program at the American University of Sharjah (AUS). During his Masters, he published work on improving DC modeling of HEMT and FET transistors. Later, he worked as a Guest

In-Residence Researcher with the American University of Sharjah exploring behavioral modeling and deep learning techniques applied on Doherty power amplifiers and digital predistortion. His research interests include overlap between device modeling and deep neural networks and their applications in general.

OUALID HAMMI (Member, IEEE) received the B.Eng. degree from the École Nationale d'Ingénieurs de Tunis, Tunis, Tunisia, in 2001, and the M.Sc. degree from the École Polytechnique de Montréal, Montréal, QC, Canada, in 2004, and the Ph.D. degree from the University of Calgary, Calgary, AB, Canada, in 2008, all in electrical engineering.

From 2010 to 2015, he was a Faculty Member with Department of Electrical Engineering, King Fahd University of Petroleum and Minerals, Dhahran, Saudi Arabia. He is currently a Professor with the Electrical Engineering Department, American University of Sharjah, Sharjah, United Arab Emirates. Since 2015, he has been an Adjunct Professor with the Electrical and Computer Engineering Department, Schulich School of Engineering, University of Calgary, Calgary, AB, Canada. He is the coauthor of two books, more than 100 articles, and inventor/co-inventor on 13 U.S. patents. His research interests include the design of energy-efficient linear transmitters for wireless communication and satellite systems, and the characterization, behavioral modeling, and linearization of radiofrequency power amplifiers and transmitters.

LUTFI ALBASHA (Senior Member, IEEE) received the B.Eng. (Hons.) and Ph.D. degrees in electronic and electrical engineering from the University of Leeds, U.K., and the M.Sc. degrees (Hons.) from Bradford University, U.K. He joined Sony Corporation in 1997, where he was involved in designing commercial RFIC chip products for mobile handsets. He joined Filtronic Semiconductors in 2000 as a Senior Principal Engineer, and created and managed its IC design team. The team supported the company foundry design enablement for mass production of RFIC products and taped-out its first commercial chips. This becomes a very successful business in Europe's largest GaAs MMIC foundry. He returned to Sony as the Lead Principal Engineer, and was involved in highly integrated RFCMOS and BiCMOS transceivers for cellular and TV applications. He joined the American University of Sharjah and progressed to rank of Professor of Electrical Engineering. His current research and publications include energy harvesting, wireless power transfer, implantable devices, front-end design, and miniaturized digital radar transceivers. He received many recognition awards for outstanding industrial and academic performances from Sony Corporation, the IET, IEEE, and the University of Leeds. He is an Associate Editor of the *IET Microwaves, Antennas, and Propagation Journal*. He served for three terms as the President of the UAE Chapter of the IEEE Solid-State Circuits Society.

HASAN MIR (Senior Member, IEEE) received the B.S. *(cum laude)*, M.S., and Ph.D. degrees in electrical engineering from the University of Washington, Seattle, WA, USA, in 2000, 2001, and 2005, respectively.

He was with the Air Defense Technology Group, MIT Lincoln Laboratory, from 2005 to 2009, where he was involved in several projects related to airborne and maritime radar systems. Since 2009, he has been with the Department of Electrical Engineering, American University of Sharjah, where he is currently a Professor. He serves as an Associate Editor for several journals, including the IEEE TRANSACTIONS ON AEROSPACE AND ELECTRONIC SYSTEMS and *IET Microwaves, Antennas, and Propagation*.

• • •